Plasmonics
https://doi.org/10.1007/s11468-025-03224-9

RESEARCH

Innovative Jet Plasma-Assisted Green Synthesis of TiO_2@Ag Core–Shell Nanoparticles Using Chard Leaf Extract for Antibacterial Applications

Zainab Fakhri Merzah[1] · Zainab J. Shanan[2] · Nisreen Kh. Abdalameer[2] · Sokina Fakhry[3]

Received: 7 June 2025 / Accepted: 15 July 2025

Abstract

This study presents, for the first time, an innovative Jet Plasma-assisted technique for the green synthesis of TiO_2@Ag core–shell nanoparticles using chard leaf extract as a natural reducing and stabilizing agent. The Jet Plasma provides a highly energetic environment that accelerates nucleation and core–shell formation at low temperatures without toxic precursors. The synthesized nanoparticles exhibited uniform and stable structures, as confirmed by comprehensive characterization techniques including X-ray diffraction (XRD), Fourier-transform infrared spectroscopy (FTIR), ultraviolet–visible (UV–Vis) spectroscopy, transmission electron microscopy (TEM), and zeta potential analysis. XRD patterns confirmed the crystalline anatase phase of TiO_2 alongside distinct metallic silver phases. TEM images revealed spherical nanoparticles with silver cores measuring 4.5–4.9 nm surrounded by TiO_2 shells of 9–13 nm thickness. Optical analysis showed a surface plasmon resonance peak at 404 nm and a TiO_2 bandgap of approximately 3.0 eV. The nanoparticles demonstrated good colloidal stability with a zeta potential of –13.5 mV and exhibited effective photocatalytic activity in the degradation of organic dyes. Antibacterial evaluation using the broth dilution method revealed potent inhibitory effects against *Staphylococcus aureus* and *Escherichia coli*, with inhibition observed at concentrations ranging from 125 to 1000 µg/mL. These findings highlight the potential of these nanostructures for sustainable water treatment and enhanced photocatalytic applications.

Highlights

- A novel, eco-friendly method was developed for synthesizing TiO_2@Ag core–shell nanoparticles using jet plasma and chard leaf extract.
- TEM analysis confirmed the formation of well-defined core–shell structures with Ag cores (4.5–4.9 nm) and TiO_2 shells (9–13 nm).
- XRD analysis revealed the anatase phase of TiO_2 and the presence of metallic silver nanoparticles.
- The synthesized nanoparticles exhibited strong UV absorption (~414 nm) with a narrow band gap (\~3.0 eV).
- The TiO_2@Ag nanostructures demonstrated excellent antibacterial activity against *E. coli* and S. *aureus*.
- The nanocomposite effectively degraded RhB dye, showing promising photocatalytic performance.

Extended author information available on the last page of the article

Published online: 29 July 2025

Graphical Abstract

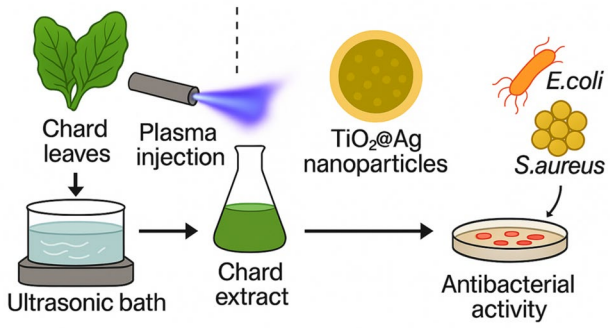

Keywords Green synthesis · Core–shell nanoparticles · Jet plasma · Chard leaf extract · Antibacterial

Introduction

Nanotechnology, which is the science of engineering and designing materials on the nanoscale, has revolutionized many areas of science by offering innovative solutions to complex world issues. Nanoparticles, a substance with one dimension within the size range of 1 to 100 nm have been the cornerstone of this technological revolution. In medicine, nanotechnology has developed nanomedicine, a revolutionary approach aimed at the diagnosis, therapy, and monitoring of various diseases with unprecedented precision. These nanoscale structures provide new paradigms to overcome many of the pharmacological limitations and optimize the efficacy, delivery, and bioavailability of therapeutic drugs in numerous various pathological conditions [1]. The creation and modification of atomic or molecular materials, frequently smaller than 100 nm, is the focus of the multidisciplinary scientific area of nanotechnology. This technology's capacity to investigate and regulate at the atomic or molecular level in the disciplines of optics, electronics, and optoelectronic devices, as well as numerous biomedical applications including radiation enhancement and gene transfer, makes it significant in a variety of applications. It is possible to further modify nanomaterials that range in size from 1 to 100 nm [2]. Improved absorption capacity and surface-to-volume ratio (and consequently surface energy) have resulted from size reduction to the nanoscale. as well as biological efficacy [3, 4]. Additionally, nanomaterials have greatly increased optical, magnetic, and thermal capabilities, as well as their physical and chemical characteristics, including permeability, durability, coloring, and solubility [5]. Along with their low density, nanoparticles also have special kinetic, mechanical, and chemical stability. Compared to their bulk/massive counterparts, novel nanomaterials and nanocomposites unquestionably provide a greater range of applications and better performance [6]. Nanotechnology It is employed in many different fields, such as energy, chemicals, cosmetics, and healthcare [7, 8]. Plasmonic nanoparticles play a vital role in extending light absorption and promoting the generation of reactive oxygen species, thereby accelerating pollutant degradation and microbial inactivation. This forms the foundation for developing multifunctional advanced nanomaterials [9]. One essential industrial ingredient found in paints, pigments, cosmetics, and other goods is titanium dioxide (TiO_2) [5]. It is also utilized in beam splitters, optical coatings, and anti-reflective coatings because of its high refractive index and dielectric stability [10]. Numerous techniques, such as chemical vapor deposition, hydrothermal synthesis, solvent thermal synthesis, gel synthesis, and green synthesis, can be used to create titanium dioxide nanoparticles [11]. The integration of silver nanoparticles into TiO_2 matrices significantly boosts the degradation of organic pollutants and effectively inhibits bacterial growth, indicating strong potential for wastewater treatment technologies [12]. The class of nanoparticles with the quickest rate of growth is silver nanoparticles (AgNPs). Because of their various biological characteristics, these noble metal nanoparticles have been the subject of much research [11, 13]. The organic production of silver nanoparticles in the medical field has made use of their anticancer, drug-carrying, diagnostic, antibacterial, antifungal, antiviral, antioxidant, and anti-inflammatory qualities [14]. Silver nanoparticles have the ability to block essential bacterial enzymes, disrupt the bacterial plasma membrane, which causes the bacteria to lose their cytoplasmic contents, or stabilize DNA replication [15]. For many years, silver nanoparticles have been recognized for their antibacterial properties against a variety of bacterial species [16, 17]. When bacteria are directly exposed to silver nanoparticles, the

antibacterial qualities of the generated particles are shown [13].They have created and implemented core–shell nanoparticles [18]. In recent decades, their many applications in chemical catalysis, biomedical drug delivery, giant magnetoresistance (GMR) sensing, and environmental remediation have garnered a lot of interest [19]. Recent studies demonstrate that combining titanium dioxide with silver or other noble metals enhances charge separation and light absorption, leading to improved degradation of organic pollutants and antibacterial activity under visible light. This advancement is crucial for addressing environmental pollution and antibiotic resistance [20]. Core–shell nanoparticles have been found to be superior to conventional nanoparticles, particularly in biological applications, due to their higher dispersibility, biocompatibility, and cytocompatibility, as well as their high chemical and thermal stability, high ability to conjugate with other types of biologically active molecules, and lower toxicity to human cells [21]. Research highlights the effectiveness of green-synthesized core–shell nanoparticles, which exhibit high stability and biocompatibility. Their controlled release of reactive oxygen species and silver ions significantly enhances photocatalytic and antibacterial performance, contributing to sustainable environmental and medical solutions [9]. Recent studies have demonstrated that green synthesis methods for core–shell nanoparticles not only improve photocatalytic efficiency but also enhance antibacterial performance, making them ideal for environmental applications [22]. For instance, plant extracts from peels, leaves, flowers, stems, buds, and pollen are used in green synthesis, a method that is good for the environment [23]. Because it does not require costly equipment, hazardous chemicals, or high temperatures, it is among the most beneficial physical and chemical procedures [24]. A variety of plant parts, including the stem, leaf, flower, and peel, serve as oxidizing, reducing, and capping agents to control the aggregation and agglomeration of nanoparticles [25]. In the process of creating nanoparticles, plant extracts may serve as capping and reducing agents. Enzymes, proteins, amino acids, vitamins, polysaccharides, and organic acids like citrate are examples of biomolecules found in plant extracts that can be used to bioreduce metal nanoparticles in a way that is safe for the environment and the environment [11]. Green synthesis approaches using plant extracts have gained significant attention for producing nanoparticles with high efficiency in catalytic and antibacterial applications. These sustainable methods offer promising avenues for water purification and advanced biomedical uses [26]. Thakur et al. demonstrated that triple doping of Co–Ni–Zn TiO_2 notably enhances photocatalytic degradation efficiency of organic pollutants under UV irradiation [27]. Similarly, Balkrishna et al. highlighted the efficacy of silver nanoparticles synthesized via plant extracts in medical and environmental applications, emphasizing the importance of natural sources in nanomaterial fabrication [28]. Other studies have shown that iron oxide nanoparticles doped with zinc and cobalt prepared by plant extracts improve nanomaterial properties and broaden their applications [29], while advanced synthesis techniques such as microwave-assisted methods have been proven to enhance characteristics of doped zinc oxide nanoparticles [30]. One of the several uses of cold plasma in material surface treatment is the production of supported metal nanoparticles [31, 32]. Cold plasma can reduce noble metal nanoparticles in a number of ways, including (1) being environmentally friendly because it does not require chemical reducing agents or reducing agents that are bad for the environment or biology; (2) operating at room temperature; (3) operating without impurities; (4) having a uniform distribution and small diameter of metal nanoparticles; (5) being economical; and (6) being simple to immobilize and stabilize between metal nanoparticles and supporting material surfaces. In general, there are several methods for creating cold plasma for materials treatment, including discharge plasma, glow plasma, and microwave radiation plasma. Plant extracts have been extensively studied as a safer substitute for traditional methods in the production of metal oxide nanoparticles [33]. The presence of harmful bacteria in contaminated water poses a serious environmental and health concern, necessitating advanced antibacterial solutions. Conventional methods often rely on toxic chemicals or energy-intensive processes, which are not environmentally sustainable. This study introduces a green synthesis approach for TiO_2@Ag core–shell nanoparticles utilizing chard leaf extract as a natural reducing and stabilizing agent, combined with jet plasma technology. Chard leaf extract was chosen due to its rich content of natural phytochemicals such as polyphenols, flavonoids, and organic acids, which act as effective reducing and stabilizing agents during nanoparticle synthesis. Additionally, chard is widely available, renewable, and has not been previously reported for the synthesis of TiO_2@Ag core–shell nanoparticles, enhancing the originality of this work. This innovative method replaces hazardous chemicals with an eco-friendly alternative while employing plasma assistance to enhance synthesis efficiency and nanoparticle quality under mild conditions. The resulting nanostructures demonstrate superior antibacterial activity and photocatalytic performance, highlighting their potential for applications in biomedical and environmental remediation. The primary aim of this research is to develop an environmentally sustainable and effective method for fabricating multifunctional TiO_2@Ag core–shell nanoparticles. By leveraging jet plasma technology, the synthesis is facilitated at low temperatures without toxic reagents, enabling the production of advanced nanomaterials with enhanced antibacterial and photocatalytic properties suitable for diverse applications in environmental

Table 1 Chemicals used for the synthesis of TiO_2@Ag core–shell nanoparticles

Chemical name	Chemical formula	Grade	Purity	Manufacturer/source
Titanium isopropoxide	$C_{12}H_{28}O_4Ti$	-	-	DIREVO Industrial Biotech, Germany
Ethanol	C_2H_5OH	AR	99%	Local supplier (Brazil origin)
Sodium hydroxide	NaOH	AR	≥98%	Merck (Germany)
Silver nitrate	$AgNO_3$	AR	≥99%	Millipore Sigma (USA)
Deionized water	H_2O	-	-	Prepared in the laboratory
Chard leaf extract	-	-	-	Fresh chard leaves were collected from a local market in Baghdad, Iraq

and biomedical fields. To the best of our knowledge, this is the first report on the jet plasma-assisted green synthesis of TiO_2@Ag core–shell nanoparticles using chard leaf extract. This novel approach offers a sustainable and efficient route to fabricate multifunctional nanomaterials with superior antibacterial and photocatalytic performance, which are highly desirable for environmental remediation and biomedical applications.

Specific Research Questions

Building upon the stated research objectives, this study seeks to address the following specific questions:

1. To what extent can jet plasma technology facilitate the environmentally sustainable synthesis of TiO_2@Ag core–shell nanoparticles with controlled morphology and composition?
2. What are the detailed structural, morphological, and optical properties of the synthesized TiO_2@Ag nanoparticles?
3. How effective are the synthesized TiO_2@Ag nanoparticles in inhibiting pathogenic bacteria commonly found in contaminated water?
4. What is the photocatalytic efficiency of these nanoparticles in degrading organic pollutants under simulated environmental conditions?

Materials and Methods

Materials

Used in this study, titanium isopropoxide ($C_{12}H_{28}O_4Ti$) (DIREVO Industrial Biotech, Germany), deionized water, 99% pure ethanol (Eth) from Brazil, sodium hydroxide (NaOH), silver nitrate ($AgNO_3$), and extract from chard leaves, and the supplier of each chemical is presented in Table 1. Ample preparation was conducted using a centrifuge (model 5804R, China), drying oven (model DHG-9030A, China), and a furnace for calcination (locally fabricated, Iraq).

Method

Preparation of Chard Leaf Extract

The extraction process began by washing the chard leaves three times with tap water to remove dust and impurities, followed by a final rinse with distilled water to ensure optimal cleanliness. Excess moisture was removed by gently shaking the leaves, which were then chopped and left to dry at room temperature, away from direct sunlight, for 5 days. After drying, the leaves were ground into a fine powder using a household electric grinder. Precisely, 5 g of the powdered leaves was weighed and mixed with 100 ml of deionized water in a glass beaker. The mixture was stirred continuously for 30 min at 70 °C using a magnetic stirrer to facilitate the extraction of bioactive compounds. After stirring, the extract was centrifuged at 5000 rpm for 30 min to remove suspended impurities and particulates. Finally, the clear supernatant is filtered through Whatman No. 1 filter paper to obtain a purified green aqueous extract, as illustrated in Fig. 1. The extract was stored in a cool, dry place until used for the synthesis of TiO_2@Ag core–shell nanoparticles.

Jet Plasma-Assisted Green Synthesis of TiO_2@Ag Core–Shell Nanoparticles

The preparation steps are shown in Fig. 2. Initially, 50 ml of deionized water was mixed with 26.5 ml of titanium isopropoxide (TTIP), and the resulting mixture was placed on a magnetic shaker and stirred continuously for 30 min to ensure complete homogenization and hydrolysis of TTIP. Separately, 100 ml of deionized water containing 0.17 ml of silver nitrate was prepared and stirred on a magnetic shaker for 10 min to dissolve the silver salt uniformly. Subsequently, 10 ml of the silver nitrate solution was taken, and 50 ml of chard leaf extract was gradually added dropwise under constant stirring to facilitate the reduction of silver ions by the phytochemicals present in the extract. Following this, 10 ml of the previously prepared TTIP solution was added dropwise to the mixture of silver nitrate and leaf extract to initiate the formation of the TiO_2@Ag precursor. After 5 min of continuous stirring on the magnetic shaker,

Fig. 1 Stepwise preparation of chard leaf extract used in nanoparticle synthesis

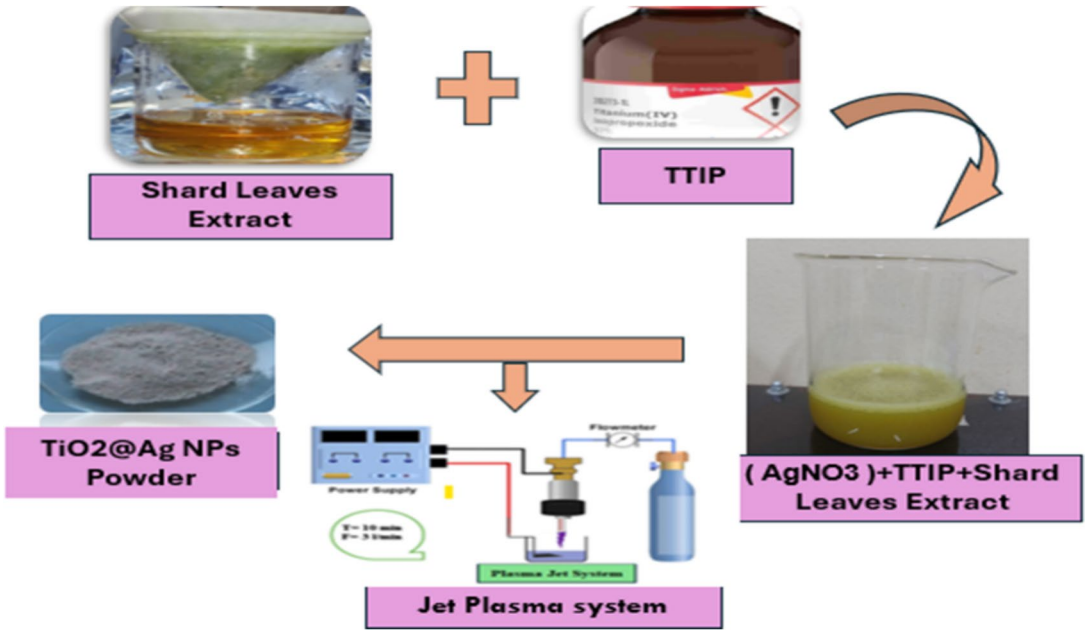

Fig. 2 Schematic illustration of TiO_2@Ag core–shell nanoparticle synthesis assisted by jet plasma

the mixture was subjected to jet plasma treatment. A volume of 10 ml of the solution was transferred into a glass beaker positioned directly beneath the plasma system electrodes, where the inter-electrode distance had been carefully adjusted to optimize plasma exposure during a 2-min plasma treatment, argon gas was flowed through the system at a rate of 5 l/min into the beaker. The application of a high potential electrical difference ionized the argon gas molecules, generating reactive oxygen and nitrogen species such as ozone and hydroxyl radicals [34, 35]. These reactive species facilitated the formation of monovalent TiO_2@Ag nanoparticles with a core–shell structure. The jet plasma also provided a charged environment that stabilized the nanoparticles, preventing agglomeration and maintaining their nanoscale size, as described in [24]. Finally, the synthesized nanoparticles were separated by centrifugation at 4000 rpm for 20 min, followed by drying in an oven at 400 °C for approximately 6 h to obtain the final TiO_2@Ag core–shell nanoparticles. The final obtained TiO_2@Ag core–shell nanoparticles weighed approximately 1.5 g, corresponding to a synthesis yield of around 30% based on the initial mass of starting materials.

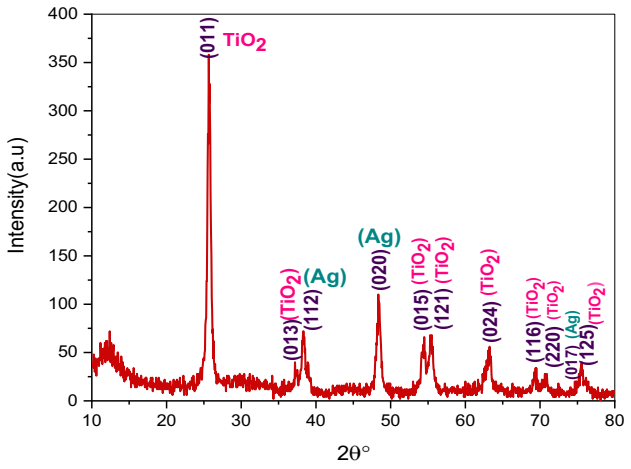

Fig. 3 XRD analysis of TiO_2@Ag core–shell nanoparticles synthesized using jet

Results and Discussions

XRD Analysis of Crystalline Structure

X-ray diffraction (XRD) is used to analyze the crystalline structure of solids with high precision. This technique relies on measuring the diffraction pattern resulting from the interference of X-rays with the atomic planes within the material. Figure 3 shows the phases of the TiO_2@Ag core–shell NP sample prepared by the green method using chard leaf extract and jet plasma. The anatase phase of TiO_2 exhibits eight Bragg diffraction lines at $2\theta = 25.427°$, 37.237°, 54.397°, 55.309°, 63.126°, 69.417°, 70.608°, and 75.630°, in the tetragonal phase, according to the card type (JCPDS 98–015-4609). Furthermore, three Bragg diffraction lines at $2\theta = 38.784°$, 48.240°, and 74.859° were found for the silver phase. TiO_2 peaks appear more clearly in XRD than Ag due to their larger crystallite size and higher silver content, as well as the effect of TiO_2 coating, which attenuates the intensity of the silver peaks. The increased crystallinity of TiO_2 reveals the strength and sharpness of the peaks. TiO_2 peaks appear more clearly in XRD than Ag due to their larger crystallite size and higher silver content, as well as the effect of TiO_2 coating, which attenuates the intensity of the silver peaks. The increased crystallinity of TiO_2 reveals the strength and sharpness of the peaks [36]. These results demonstrate the ability of the green method to produce a pure material with regular crystalline properties, increasing its potential for use in pharmaceutical and environmental technologies [37]. The crystallite size of the nanoparticles was determined using the Debye–Scherrer equation, represented in Eq. (1) below [37]. The distinct and sharp diffraction peaks observed in the XRD pattern confirm the high crystallinity and purity of the synthesized TiO_2@Ag core–shell nanoparticles. High crystallinity is associated with enhanced photocatalytic activity and chemical stability, which are crucial for environmental and biomedical applications. The attenuation of silver peak intensity by the TiO_2 shell indicates successful coating and core–shell formation, which can influence charge transfer processes and particle stability. Moreover, the crystallite size calculated via the Debye–Scherrer equation provides insight into the nanoscale dimensions, which are critical for tailoring the material's optical and catalytic properties.

$$D = \frac{0.9\lambda}{\beta\cos\theta} \tag{1}$$

where 0.9 is the Debye–Scherrer constant; D denotes the crystallite size; the full width half maximum (FWHM) of CuKα (β) radiation; where θ is the Bragg angle, has a wavelength of $\lambda = 0.154$ nm. Table 2 presents the structural parameters revealed by X-ray diffraction (XRD).

Estimated Specific Surface Area

The specific surface area (SSA) of the TiO_2@Ag core–shell nanoparticles was estimated assuming spherical particle morphology, using Eq. (2):

$$SSA = \frac{6}{D \times \rho} \tag{2}$$

where D is the average crystallite size in meters, obtained from XRD analysis; and $\rho\backslash rho\rho$ is the density of TiO_2, approximately 4.23 g/cm^3 (or 4230 kg/m^3). This estimation provides an approximate SSA value based on crystallite size and material density.

TEM A vital technique for describing nanomaterials is transmission electron microscopy (TEM), which provides high-resolution imaging that shows the internal structure

Table 2 Structural properties of TiO_2@Ag core–shell nanoparticles

Sample	2Θ (deg)	FWHM (deg)	*h k l*	D_{hkl} (A)	C. S
Tio_2 @Ag NPs (core shell)	25.427	1.75	(011)	3.500	5.62
	37.237	1.25	(103)	2.412	6.72
	38.784	1.04	(112)	2.319	7.51
	48.240	0.89	(020)	1.885	8.21
	54.397	0.78	(015)	1.685	9.44
	55.309	0.74	(121)	1.659	10.14
	63.126	1.09	(024)	1.471	5.81
	69.417	0.82	(220)	1.352	6.65
	70.608	0.74	(017)	1.267	7.13
	75.630	0.69	(125)	1.256	8.22

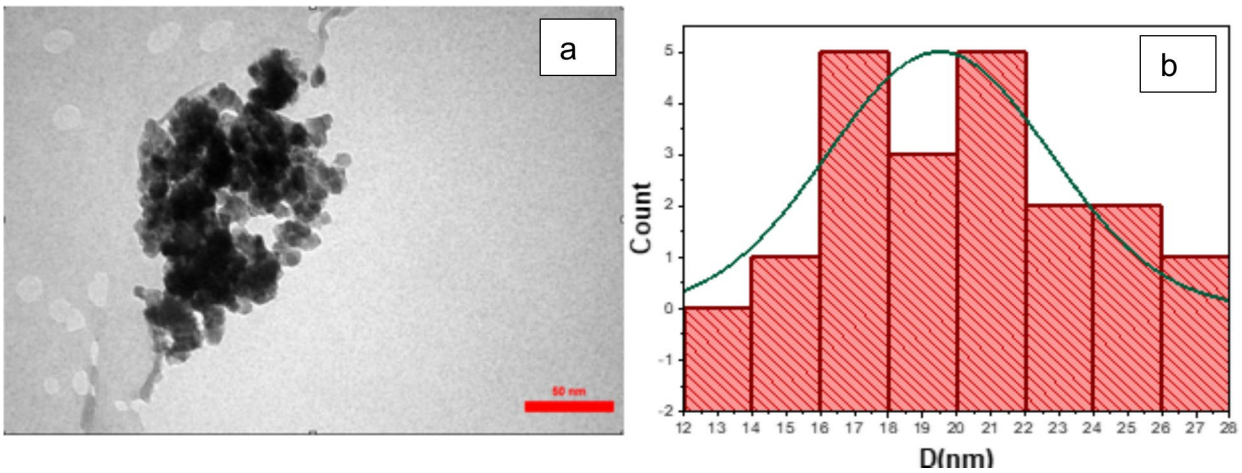

Fig. 4 **a** TEM images and **b** grain size distribution of TiO_2@Ag core–shell nanoparticles

of particles, the core–shell boundary, and the homogeneity of size and shape. TEM analysis in this study demonstrated that the TiO_2@Ag core–shell NPs are composed of (TiO_2) shell layer with a thickness of 9–13 nm encasing (Ag) core with a diameter of 4.5–4.9 nm. This confirmed the successful formation of a distinct core–shell structure. The observed core–shell morphology, characterized by a uniform TiO_2 shell enveloping the Ag core, is fundamental to the enhanced photocatalytic and antibacterial properties of the nanoparticles. The TiO_2 shell provides chemical stability and facilitates charge separation, reducing recombination of electron–hole pairs, while the Ag core offers plasmonic effects that amplify light absorption. The slight agglomeration detected is typical in nanomaterials and may influence surface-related properties; however, it does not compromise the distinct core–shell structure essential for the targeted applications. The TiO_2 shell adds to improved chemical stability and photocatalytic activity, while the Ag core offers unique plasmonic characteristics, making these nanostructure very significant photocatalytic applications. The results of this investigation are congruent with the observed values, as demonstrated by a published work that shows that multilayer coating techniques. TiO_2 shell thicknesses to about 28 nm [38]. Furthermore, the efficiency of TiO_2 deposition on Ag cores utilizing environmentally friendly techniques is supported by comparable published data. TEM pictures showed a clear shell layer with a thickness that was comparable to our findings, demonstrating the uniformity of these nanomaterials' structural behavior throughout investigation [39]. The core–shell structure is evident in the TEM image, which displays a uniform distribution of particles with a distinct electrical contrast between the low-density TiO_2 shell and the high-density Ag core shown Fig. 4 a and b. The particles do, however, exhibit some agglomeration, most likely because of weak van der Waals forces or high surface energy characteristics brought on by the nanoscale size, which cause partial fusion and particle attraction during drying or measurement preparation. The discrimination of the particles' multilayer structure was unaffected by these agglomerations, though. This improves the particles' structural composition's dependability, which is important for use in industries including photocatalysis, water purification, and nano sensing [40].

Optical Characteristics of TiO2@Ag core–shell NPs

UV–Vis technology was used to investigate the optical properties of TiO_2@AgNPs (core–shell). Figure 5 shows a significant absorption band at a wavelength of approximately 404 nm. The appearance of a faint band in the visible light absorption region between 400 and 440 nm indicates that the TiO_2@Ag core–shell NPs have a certain ability to absorb visible light. The band gap (E_g) of the synthesized material was calculated using the Kubelka–Munk (K-M) theory [30]. The band gap of TiO_2@Ag core–shell NPs is 3 eV. This gap was calculated using Eq. (3):

$$E_g = \frac{hc}{\lambda} = \frac{1240}{\lambda} \tag{3}$$

In this case, c is the speed of light (3×10^8 m/s); h is Planck's constant = ($6.626 \times 10^{\times 34}$ J/s), E_g is the band-gap energy, and λ_{max} is the wavelength, which is at the highest wavelength of the absorption spectrum [41]. The Kubelka–Munk function is widely used to estimate the optical band gap of semiconductor powders from diffuse reflectance spectra. Accurate determination of the band gap requires correct identification of the type of electronic transition (direct or indirect), as misinterpretation can lead to incorrect values affecting material analysis. Moreover, electron–hole recombination significantly influences the

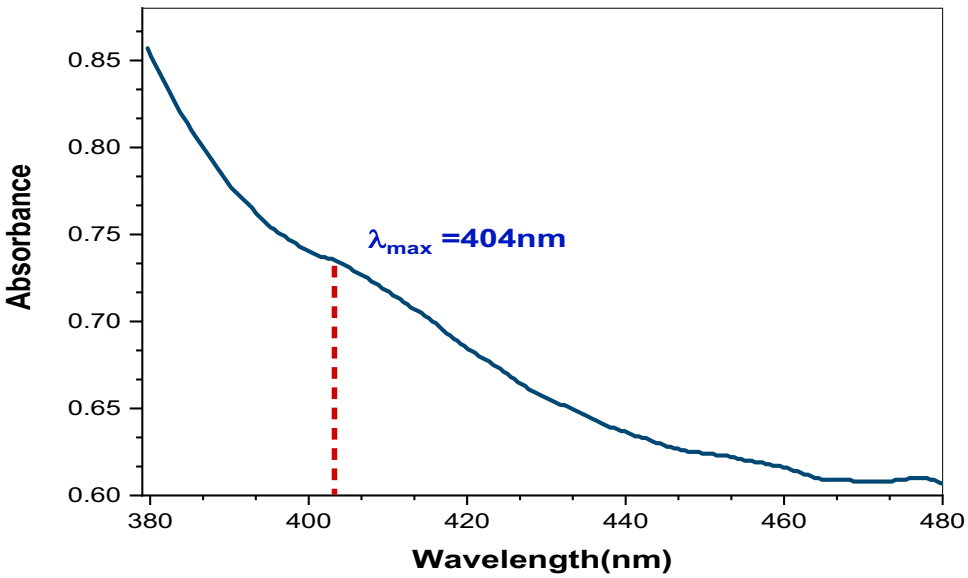

Fig. 5 UV–Vis absorption spectrum of TiO_2@Ag core–shell nanoparticles

photocatalytic efficiency of semiconductor nanomaterials by reducing charge carrier lifetime. Techniques such as X-ray photoelectron spectroscopy (XPS) are essential to analyze recombination mechanisms and surface states, thereby providing insights into optimizing material properties [42]. XPS further enables detailed characterization of surface defects and electronic states that contribute to recombination, guiding synthesis improvements to enhance photocatalytic and antibacterial performance [43]. The generation of new energy levels within the bandgap of titanium dioxide (TiO_2) because of interactions with silver particles causes a smaller energy gap in the TiO_2@Ag core–shell NPs, allowing for the absorption of visible light. Furthermore, silver increases photoactivity by enhancing the surface plasmon resonance property. This property has led to the use of the nanomaterial as an antibacterial [44].

FTIR Spectral Analysis of TiO_2@Ag Core–Shell Nanoparticles

The functional groups that had a clear role in the stability and biogenesis of the nanoparticles were quantified using Fourier transform infrared (FTIR) spectroscopy (Figure 6). The findings demonstrated that TiO_2@Ag core–shell NPs and chard leaf extract had certain functional groups in common. In all three samples, these functional groups contained the wide O–H stretching absorption band at about 3428.98 cm^{-1}. These functional groups for the vibration of alcohols or water [45]. When the plant extracts and nanoparticles were analyzed, the C–H groups were identified as the source of the stretching absorption bands at 2956.82, 2924.19, and 2853.57 cm^{-1} [46]. The carbonyl ester groups, or C–O groups, were identified as the source of the stretched absorption bands at 2361.52, 2349.65, 2336.16, and 1738.67 cm^{-1} [47]. Additionally, at about 1631.76 cm^{-1}, C–C stretched absorption bands were found. As a result, interactions with C–C groups affected how the nanoparticles formed. Furthermore, an absorption band showed at 1466.82, 1384.92, 1271.36, and 1111.28 cm^{-1}, which was ascribed to the Ti-O groups' vibration [48]. Nonetheless, any peaks that show up below 796.83 and 672.51 cm^{-1} are indicative of bonding groups in TiO_2 nanoparticles with vibrational peaks (Ti–O–Ti) as a fingerprint [49]. Ag bonding groups are indicated by peaks that show above 619.77 cm^{-1} [46]. Based on the study by Anwar et al. (2024), the functional groups present in chard leaf extract were identified using FTIR analysis, which helps to understand their role in nanoparticle synthesis and interaction with metal ions [50]. The appearance of distinct peaks in the FTIR spectrum is strong evidence of the successful preparation of TiO_2@AgNPs (core–shell) using chard leaf extract with jet plasma. The peaks of the plant functional groups indicate the immobilization of bioactive compounds on the surface of the nanoparticles, which enhances stability and green synthesis. In addition, the appearance of distinct peaks at lower ranges (typically between 500 and 800 cm^{-1}) are attributed to the vibrations of Ti–O and Ag, clearly indicating the formation of titanium oxide and silver nanoparticles [51]. The appearance of characteristic peaks for O–H stretching (3400 cm^{-1}) and C=O stretching (1600 cm^{-1}) indicates the presence of polyphenols and flavonoids, further confirming the successful structural preparation of TiO_2@Ag core–shell NPs. The presence of these functional groups, particularly hydroxyl, carbonyl, and Ti–O vibrations, plays a crucial role in the stabilization and biofabrication of the TiO_2@Ag core–shell nanoparticles. These groups facilitate strong interactions between the plant extract biomolecules and the nanoparticle surface, enhancing nanoparticle dispersion, preventing aggregation, and

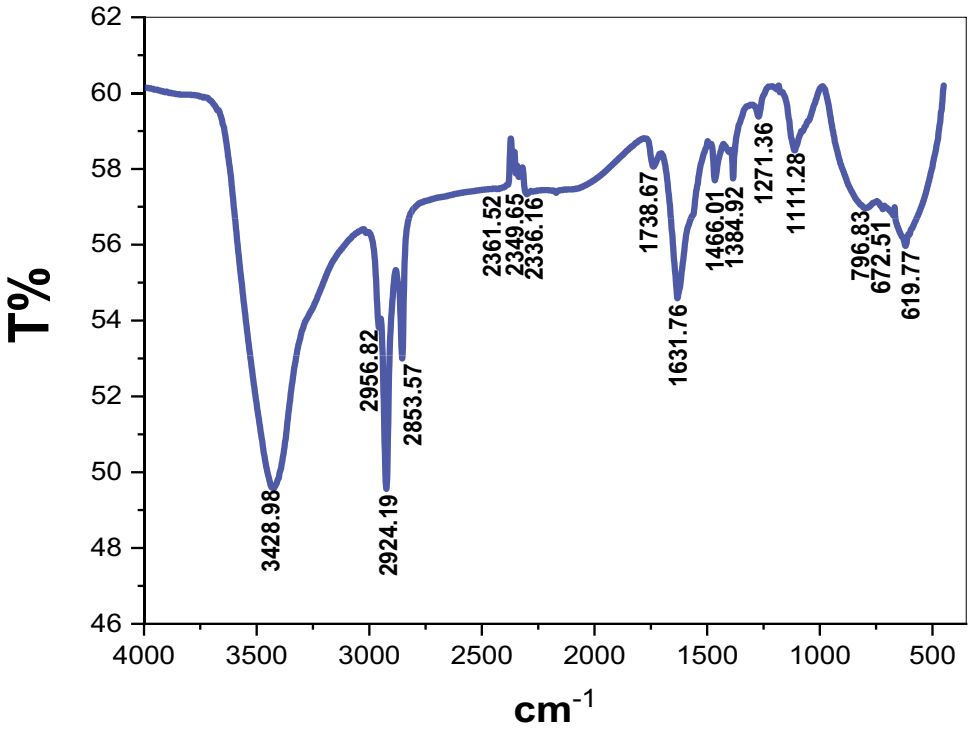

Fig. 6 FTIR spectrum of TiO_2@Ag core–shell nanoparticles

contributing to the environmentally friendly green synthesis process. Moreover, the characteristic peaks confirm the successful integration of silver and titanium oxide phases, which is essential for the nanoparticles' photocatalytic and antibacterial functionalities. Table 3shows functional groups found in TiO_2@Ag core–shell NPs.

Zeta Potential Analysis

Zeta potential measurements were performed to verify the surface charge and stability of the synthesized nanoparticles. This nanomaterial exhibits a positive zeta charge, indicating repulsion between the nanoparticles, according to the zeta potential studies shown in Fig. 7. Repulsion between the nanoparticles is beneficial for preventing agglomeration and sedimentation from the suspension. For nanoparticles containing TiO_2@Ag core–shell NPs, a zeta potential value of − 20 mV is believed to constitute the steady-state condition. Due to Vander Waals interactions between the nanoparticles, which cause agglomeration or clustering. According to recent studies, particles with zeta potentials greater than + 30 mV or less than − 30 mV are often more stable [52]. The results showed that this nanomaterial has − 13.5 zeta potential. The zeta potential value of − 13.5 mV indicates moderate stability of the nanoparticles. While it is below the commonly accepted threshold of ± 30 mV for strong electrostatic repulsion, it still provides sufficient repulsive forces to reduce excessive aggregation. This level of stability is acceptable for practical applications, although further surface modification may enhance dispersion and long-term stability, which is important for the stability of nanoparticles, compared to other materials. Currently,

Table 3 Functional groups identified in TiO_2@Ag core–shell nanoparticles

Functional group	TiO_2@Ag core–shell NPs wave number (cm^{-1})	Reference number
O–H	3428.98	[29]
C–H	2956.82, 2924.19, and 2853.57	[30]
C–O	2361.52, 2349.65, and 2336.16	[31]
C–C	1738.67 and 1631.76	[31]
Ti–O	1466.01, 1384.92, 1271.36, and 1111.28	[34]
Ti–O–Ti	796.83 and 672.51	[33]
Ag	619.77	[34]

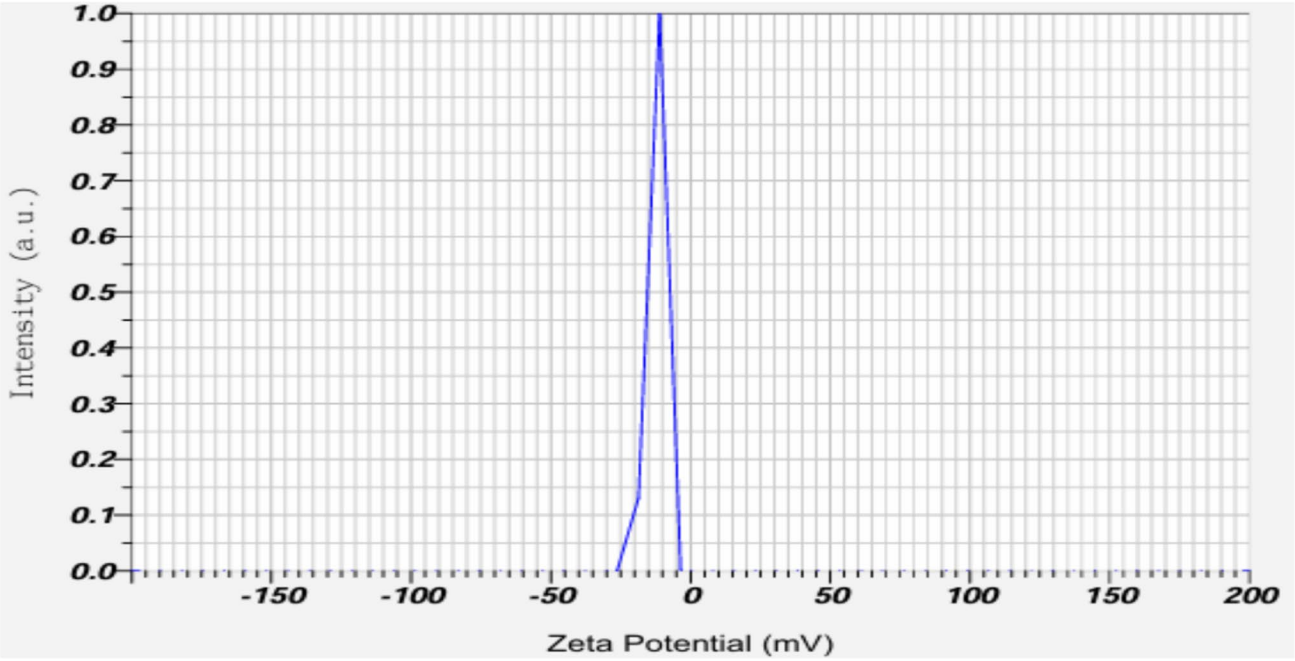

Fig. 7 Zeta potential analysis of TiO_2@Ag core–shell nanoparticles

coatings resistant to bacteria and other microorganisms are being made using TiO_2@Ag core–shell NPs. The zeta potential of the nanoparticles helps repel bacteria and other particles from the coated surface [53, 54].

Bacterial Activity Assessment

For many years, TiO_2 has been the most widely used semiconductor metal oxide photocatalyst due to its strong oxidizing properties and affordable price [8], biocompatibility, and long-term photostability. It is commonly known that pure TiO_2 works effectively against both Gram-positive and Gram-negative bacteria [55, 56]. Through the use of transition metals like silver or non-metal ions like carbon or nitrogen, several techniques were employed to re-engineer and broaden the large bandgap of TiO_2 toward the photocatalyst's light absorption into the visible range. Likewise, doping TiO_2 with silver nanoparticles or carbon and nitrogen [57, 58]. The TiO_2@Ag core–shell nanoparticles exhibit dual functionality arising from the synergistic interaction between their components. The TiO_2 shell acts as a photocatalyst, generating reactive oxygen species (reactive oxygen species — ROS) such as hydroxyl radicals (·OH), superoxide anions ($O_2{\cdot}^-$), and hydrogen peroxide (H_2O_2) under light irradiation. These species effectively degrade pollutants and inactivate bacteria. Meanwhile, the Ag core provides strong antimicrobial activity through the sustained release of Ag^+ ions that disrupt bacterial cell membranes, proteins, and DNA. This core–shell structure enhances charge separation and ROS generation via plasmonic resonance, leading to improved photocatalytic and antibacterial performance. This mechanism is supported by Liu et al., who demonstrated that such heterostructures show enhanced visible-light photocatalytic and antimicrobial activity due to interfacial charge transfer and plasmonic effects [59]. The biosynthetic synthesis using chard leaf extract offers a green alternative to conventional methods by avoiding toxic chemicals and reducing energy consumption. Combined with jet plasma assistance, this approach enhances synthesis efficiency under mild, eco-friendly conditions, promoting sustainable production of TiO_2@Ag core–shell nanoparticles suitable for environmental and biomedical applications. The antibacterial activity of TiO_2@Ag core–shell nanoparticles results from a synergistic combination of mechanisms from both TiO_2 and Ag counterparts. The TiO_2 shell generates electron–hole pairs (e^-/h^+) upon light irradiation owing to its photocatalystic property. These charge carriers interact with water and oxygen molecules adsorbed on the nanoparticle surface and produce reactive oxygen species (ROS), such as hydroxyl radicals (·OH), superoxide anions (O_2^-), and hydrogen peroxide (H_2O_2). These ROS are highly reactive and are able to damage vital biomolecules, such as lipids, proteins, and nucleic acids, inducing oxidative stress and bacterial cell death. At the same time, the Ag core is also responsible for the antibacterial activity by donating Ag^+ ions to the medium. Silver ions are established to have

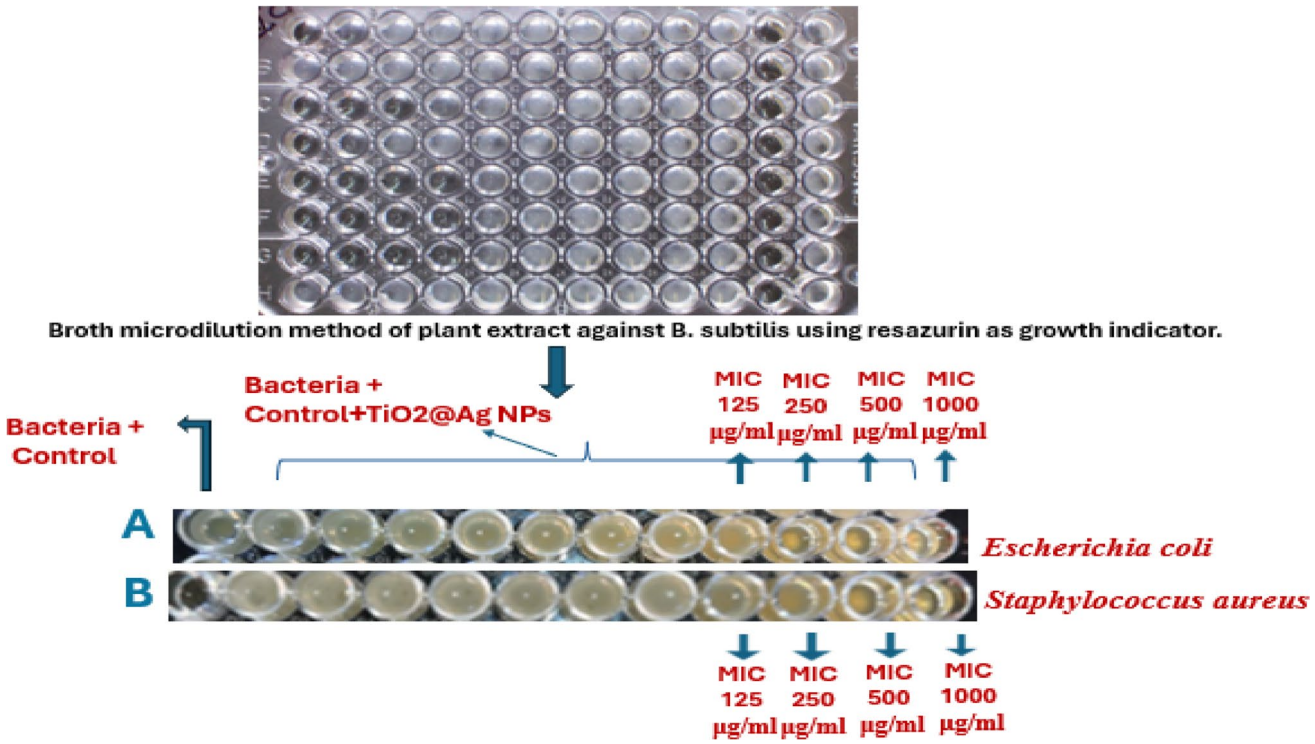

Fig. 8 Antibacterial activity of TiO_2@Ag nanoparticles assessed by minimum inhibitory concentration (MIC) against **A** *Staphylococcus aureus* and **B** *Escherichia coli*

broad-spectrum antimicrobial effects. They chelate with thiol groups in bacterial proteins and enzymes, cause inhibition of respiration, and interfere with membrane integrity. Ag^+ ions also increase membrane permeability, causing leakage of intracellular contents. The synergistic interaction of ROS formation by TiO_2 and release of Ag^+ from the metallic core enhances the bactericidal activity of the nanocomposite. The dual mechanism not only increases the rate of bacterial killing but also decreases the likelihood of resistance development, and thus TiO_2@Ag core–shell nanoparticles are a promising candidate for biomedical applications [1, 60, 61].

Broth Dilution Method (MIC)

Microscopic or complete broth dilution is one of the simplest methods for detecting antimicrobial resistance using a 96-well microtiter plate. The minimum inhibitory concentration (MIC) is the concentration of an antimicrobial agent that, when seen with the naked eye, totally stops the growth of the organism in tubes or microdilution wells. Both antifungal and antibacterial microdilution assays frequently use viewing devices to help establish the MIC endpoint because they make it easier to examine microdilution tests and record data with a high ability to notice growth in the wells [62]. A stock solution of TiO_2@Ag core–shell nanoparticles (1000 µg/ml) was prepared by dissolving 1 g of the nanoparticles in 10 ml of distilled water. These nanoparticles are then used in the broth dilution assay, as shown in Fig. 8, to evaluate their inhibitory activity against *Staphylococcus aureus* and *Escherichia coli*. You should add this paragraph right after the part where you describe the MIC results and bacterial inhibition concentrations (i.e., after the sentences discussing Fig. 8 and inhibition levels against *Staphylococcus aureus* and *Escherichia coli*). This will smoothly expand your discussion by interpreting and contextualizing the results. Inhibition of *Escherichia coli* was observed at concentrations of 1000, 500, 250, and 125 µg/ml using the broth dilution method (MIC). This method demonstrated effective bacterial growth suppression across these concentrations for both *Escherichia coli* and *Staphylococcus aureus*. The broth dilution assay provided clear evidence of gradual inhibition, confirming its efficacy in evaluating antibacterial activity. Compared to previously reported methods for synthesizing TiO_2@Ag or similar core–shell nanoparticles, the present study offers several advantages. Traditional chemical methods often require toxic reducing agents and high-temperature conditions, whereas our approach uses a non-toxic, plant-based extract (chard leaf) under mild conditions, assisted by jet plasma to enhance synthesis efficiency and nanoparticle quality. For example, Nabi et al. reported the green

synthesis of TiO_2 nanoparticles using lemon peel extract, achieving significant photocatalytic activity. However, the current method not only avoids hazardous reagents but also integrates silver to enhance antibacterial functionality, providing a multifunctional material suitable for environmental remediation [63].

Limitations and Contributions

Although this study presents an innovative and green synthesis method for TiO_2@Ag core–shell nanoparticles with enhanced antibacterial properties targeting bacterial inhibition in contaminated water, certain limitations remain. The scalability of the jet plasma-assisted synthesis technique requires further investigation to assess its feasibility for large-scale production. Additionally, long-term stability tests and comprehensive studies are needed to evaluate the nanoparticles' effectiveness across various and dynamic polluted water conditions. Despite these limitations, this work makes a significant contribution by being the first to apply a sustainable, plasma-assisted green synthesis approach using chard leaf extract. The developed nanomaterials demonstrate excellent performance in inhibiting harmful bacteria, showing great promise for applications in polluted water treatment and environmental remediation.

Conclusions

In this study, TiO_2@Ag core–shell nanoparticles were successfully synthesized via a green method using chard leaf extract combined with jet plasma assistance. Characterization results confirmed the nanoscale crystalline structure, as evidenced by XRD analysis, which revealed the anatase phase of TiO_2 and distinct silver phases. FTIR spectra demonstrated the presence of Ti–O and Ag bonds alongside functional groups from the plant extract, validating the green synthesis approach. The nanoparticles exhibited an energy bandgap of approximately 3.0 eV, according to UV–Vis spectroscopy. TEM images showed a core–shell morphology, with a silver core measuring 4.5–4.9 nm enveloped by a TiO_2 shell of 9–13 nm thickness. Zeta potential analysis indicated moderate stability with values around − 13.5 mV. Antibacterial tests using the broth dilution method (MIC) revealed significant inhibitory effects against *Escherichia coli* and *Staphylococcus aureus*, highlighting the potential of these nanostructures for biomedical applications. The new conclusion articulates the worldwide problem addressed in this research clearly: the need for environmentally safe, sustainable, and effective antibacterial agents to combat drug-resistant bacteria. This work demonstrates a novel and eco-friendly synthesis approach of multifunctional TiO_2@Ag core–shell nanoparticles that exhibit simultaneous photocatalytic and antibacterial activity. The outcomes, while predictable, provide a scalable and green synthesis route that addresses both environment and biomedical concerns. Future researches will focus on streamlining this process for industrial applications and in vivo efficacy testing.

Acknowledgements Authors offer their deep gratitude to the Lab. Nano, Departments of physics, and College of Science for Women, University of Baghdad, for their support and advice.

Author Contribution Zainab F. M: Data curation, Writing–review and editing., Z.J.Sh: Conceptualization, Investigation, Methodology. Zainab F. M: Project administration, Supervision, Nisreen Kh. Abdalameer: Visualization, Writing – original

Data Availability No datasets were generated or analysed during the current study.

Declarations

Ethics Not applicable.

Conflicts of interest The authors declare that they have no conflict of interest.

Statement of Usage of Artificial Intelligence The authors declare that no artificial intelligence was used in writing the research paper.

References

1. Abadi EHL, Amiri M, Ranaee M et al (2025) Plasmonic selenium nanoparticles biosynthesized from Crataegus monogyna fruit extract: a novel approach to mitigating chromium-induced toxicity. Plasmonics 20:3805–3815. https://doi.org/10.1007/s11468-024-02539-3
2. Sahani S, Sharma YC (2021) Advancements in applications of nanotechnology in global food industry. Food Chem 342:128318
3. Negi G, Anirbid S, Sivakumar P (2021) Applications of silica and titanium dioxide nanoparticles in enhanced oil recovery: promises and challenges. Petroleum Res 6(3):224–246
4. Shaker DS, Abass NK, Ulwali RAU (2022) Preparation and study of the structural, morphological and optical properties of pure tin oxide nanoparticle doped with Cu. Baghdad Sci J 19(3):0660–0660
5. Abdalameer NK, Fahad OA, Khalaph KA (2022) Effect of pulsed laser frequency on CdTe deposited as solar cells device. Int J Nanosci 21(01):1–8. https://doi.org/10.1142/S0219581X21500629
6. Pourpasha H, Zeinali Heris S, Mohammadfam Y (2021) Comparison between multi-walled carbon nanotubes and titanium dioxide nanoparticles as additives on performance of turbine meter oil nano lubricant. Sci Rep 11(1):11064
7. Hakeem HS, Abbas NK (2021) Preparing and studying structural and optical properties of Pb1-xCdxS nanoparticles of solar cells applications. Baghdad Sci J 18(3):0640–0640
8. Isam A, Shanan ZJ (2025) Microwave green synthesis of alumina nanoparticles and evaluation of their characterization and microbial effect. Nano Life 15(05):1–13. https://doi.org/10.1142/S1793984424500272
9. Verma N et al (2025) Photocatalytic, antibacterial and antioxidant capabilities of (Fe, Al) double doped ZnO nanoparticles with Murraya Koenigii leaf extract synthesized by using microwave assisted technique. Mater Chem Phys 333:130422

10. Shanan ZJ, Ali HMJ, Al-Taay HF (2022) Evaluation of the influence of the number of laser shots on the characterization of TiO2/MgO nanocomposites. Iran J Mater Sci Eng 19(3). https://doi.org/10.22068/ijmse.2651
11. Oleiwi HF et al (2024) Comparative study of sol-gel and green synthesis technique using orange peel extract to prepare TiO2 nanoparticles. Baghdad Sci J 21(5):1702–1702
12. Ashwin B, Yardily A, Dennison MS (2025) Microwave-assisted green synthesized ZnO nanoparticles: an experimental and computational investigation. Discover Appl Sci 7(3):177
13. Aadim KA, Mazhir SN, Abdalameer NK, Ali AH (2020) Influence of gas flow rate on plasma parameters produced by a plasma jet and its spectroscopic diagnosis using the OES technique. IOP Conf Ser Mater Sci Eng 987(1):012020. https://doi.org/10.1088/1757-899X/987/1/012020
14. Shanan ZJ, Shanshool SK, Al-Taay HF, Abdalameer NK, Hadi SM (2022) Green method of CuO NPs by using Eucalyptus camaldulensis aqueous extract with cold plasma, and its effect on biofilm formation. Int J Nanosci 21(03):1–5. https://doi.org/10.1142/S0219581X2250020X
15. Noori AS et al (2022) The histological effect of activated Aloe vera extract by microwave plasma on wound healing. Chem Phys Lett 807:140112. https://doi.org/10.1016/j.cplett.2022.140112
16. Ali HMJ, Majed MD (2024) The effect of cold plasma generated from argon gas on the optical band gap of nanostructures. Kuwait J Sci 51(2):100195.https://doi.org/10.1016/j.kjs.2024.100195.
17. Jaffer ZJ, Abdalameer NK, Noori AS (2024) Plasma surface treatment of metals: a comprehensive review of recent developments and future prospects. Int J Nanosci 23(01):2330008. https://doi.org/10.1142/S0219581X23300080
18. Serpell CJ et al (2011) Core@ shell bimetallic nanoparticle synthesis via anion coordination. Nat Chem 3(6):478–483
19. Wei S et al (2011) Multifunctional composite core–shell nanoparticles. Nanoscale 3(11):4474–4502
20. Kumar P, Arya V, Kumar A, Thakur N (2025) Polymer/phytochemical mediated eco-friendly synthesis of Cu/Zn doped hematite nanoparticles revealing biological properties and photocatalytic activity. Int J Mater Res 116(1):30–49. https://doi.org/10.1515/ijmr-2023-0343
21. Chatterjee K et al (2014) Core/shell nanoparticles in biomedical applications. Adv Coll Interface Sci 209:8–39
22. BM A, MS Dennison (2025) Integrating microwave-assisted green synthesis, DFT simulations, and biological activity evaluation of copper-doped zinc oxide nanoparticles. Scientific Reports 15(1):19348
23. Hassan AK, Atiya MA, Luaibi IM (2022) A green synthesis of iron/copper nanoparticles as a catalytic of fenton-like reactions for removal of orange G dye. Baghdad Sci J 19(6):1249–1249
24. Iravani S (2011) Green synthesis of metal nanoparticles using plants. Green Chem 13(10):2638–2650
25. Davar F, Majedi A, Mirzaei A (2015) Green synthesis of ZnO nanoparticles and its application in the degradation of some dyes. J Am Ceram Soc 98(6):1739–1746
26. Sharma S et al (2025) Photocatalytic, antibacterial and antioxidant study of *Vitex negundo* mediated green synthesized nickel and neodymium doped zinc oxide nanoparticles. Toxicol Environ Chem 107(1):178–206
27. Thakur N, Thakur N (2025) Photocatalytic adsorption and scavenging potential of chemical and green encapsulated anatase phase of coupled doped Zn-Co TiO2 nanoparticles. J Dispersion Sci Technol 46(7):1071–1086
28. Balkrishna A et al (2023) Synthesis, characterization and antibacterial efficacy of *Catharanthus roseus* and *Ocimum tenuiflorum*-mediated silver nanoparticles: phytonanotechnology in disease management. Processes 11(5):1479
29. Kumar P et al (2024) Water purification and biological efficacy of green synthesized Co/Zn-doped α-Fe2O3 nanoparticles. Sustainable Chemistry for the Environment 8:100160
30. Verma N, Pathak D, Thakur N (2024) Eco-friendly green synthesis of (Cu, Ce) dual-doped ZnO nanoparticles with *Colocasia esculenta* plant extract using microwave assisted technique for antioxidant and antibacterial activity. Next Materials 5:100271
31. El-Sayed MA (2001) Some interesting properties of metals confined in time and nanometer space of different shapes. Acc Chem Res 34(4):257–264
32. Mazhir SN et al (2022) ZnO: Fe3O4 nanoparticles produced by cold plasma: synthesis, characterization and anti-microbial activity. Int J Nanosci 21(03):2250021
33. Kadhim MM, Shehab MM, Abdalameer Nkh (2024) Plasma vacuum systems: a review article. MINAR Int J Appl Sci Technol 06(02):325–342. https://doi.org/10.47832/2717-8234.19.26
34. Mohammed RS, Al -Marjani MF (2025) Plasma–solution interaction as green pathway to synthesize novel hybrid nanoparticles for medical sterilization (catheter sterilization). Eur Phys J Plus 140(2):156
35. Mazhir SN et al (2022) Bio-synthesis of (Zn/Se) core-shell nanoparticles by micro plasma-jet technique. Int J Nanosci 21(05):2250041
36. Rahman M et al (2025) Optimizing the shell thickness of Ag@TiO2 nanostructures by a simple top-down method to engineer effective SERS substrates and photocatalysts. ACS Omega 10(15):14940–14948
37. Alam MW et al (2024) Facile green synthesis of α-bismuth oxide nanoparticles: its photocatalytic and electrochemical sensing of glucose and uric acid in an acidic medium. Journal of Composites Science 8(2):47
38. Parvathiraja C, Shailajha S (2023) Plasmonic core–shell nanoparticles of Ag@ TiO2 for photocatalytic degradation of rhodamine B. Appl Nanosci 13(6):3677–3692
39. Medhi R et al (2024) TiO2 core–shell and core-dual-shell nanoparticles with tunable heterojunctions and visible to near-infrared extinctions. Mater Adv 5(4):1648–1666
40. Vollath D, Fischer FD, Holec D (2018) Surface energy of nanoparticles–influence of particle size and structure. Beilstein J Nanotechnol 9(1):2265–2276
41. Hayder RA, Shanan ZJ (2024) Evaluation of green synthesized Fe_2O_3@MnO_2 (core/shell) nanoparticles as antibacterial and adsorbent material for heavy metals. E3S Web Conf 537:08020. https://doi.org/10.1051/e3sconf/202453708020
42. Selvaraj S, Sankaran D, Mani I (2025) Dye degradation using piperazine encapsulated biosynthesized iron nanoparticles. Chem Ind Chem Eng Q (00):10–10. https://doi.org/10.2298/CICEQ240904010S
43. Kumar P et al (2024) Chemical and green synthesized Co/Ni-doped hematite nanoparticles for enhancing the photocatalytic and antioxidant properties. Phys Scr 99(10):105960
44. Ahmed F et al (2021) An experimental and theoretical study on the effect of silver nanoparticles concentration on the structural, morphological, optical, and electronic properties of TiO2 nanocrystals. Crystals 11(12):1488
45. Aygun A et al (2023) Highly active PdPt bimetallic nanoparticles synthesized by one-step bioreduction method: characterizations, anticancer, antibacterial activities and evaluation of their catalytic effect for hydrogen generation. Int J Hydrogen Energy 48(17):6666–6679
46. Gnanasekaran L et al (2021) Visible light driven exotic p(CuO)-n(TiO2) heterojunction for the photodegradation of 4-chlorophenol and antibacterial activity. Environ Pollut 287:117304
47. Ahmad A, Ayub H (2022) Fourier transform infrared spectroscopy (FTIR) technique for food analysis and authentication. In:

Pathare PB, Rahman MS (eds) Nondestructive quality assessment techniques for fresh fruits and vegetables. Springer Nature Singapore, Singapore, pp 103–142. https://doi.org/10.1007/978-981-19-5422-1_6
48. Hameed YA et al (2025) Green synthesis and antimicrobial evaluation of Ag/TiO2 and Ag/SeO2 core-shell nanocomposites using *r. Officinalis* extract: a combined experimental and docking study. Inorg Chim Acta 574:122390
49. Kubiak A et al (2020) Microwave-assisted synthesis of a TiO2-CuO heterojunction with enhanced photocatalytic activity against tetracycline. Appl Surf Sci 520:146344
50. Elattar KM et al (2023) Phytogenic synthesis and characterization of silver metallic/bimetallic nanoparticles using *Beta vulgaris* L. extract and assessments of their potential biological activities. Appl Sci 13(18):10110
51. Pashaei S, Safari S, Hosseinzadeh S (2022) Green synthesis of silver nanoparticles using sugar beet leaf extracts and its antibacterial activity. Iran J Anal Chem 9(2):38–45
52. Hashemi Z et al (2023) Anticancer and antibacterial activity against clinical pathogenic multi-drug resistant bacteria using biosynthesized silver nanoparticles with *Mentha pulegium* and *Crocus caspius* extracts. Inorg Chem Commun 154:110982
53. Lek M et al (2016) Analysis of protein-coding genetic variation in 60,706 humans. Nature 536(7616):285–291
54. Ebrahimzadeh MA et al (2020) Enhanced catalytic and antibacterial efficiency of biosynthesized *Convolvulus fruticosus* extract capped gold nanoparticles (CFE@ AuNPs). J Photochem Photobiol, B 209:111949
55. Foster HA et al (2011) Photocatalytic disinfection using titanium dioxide: spectrum and mechanism of antimicrobial activity. Appl Microbiol Biotechnol 90:1847–1868
56. Cai Y, Strømme M, Welch K (2013) Photocatalytic antibacterial effects are maintained on resin-based TiO2 nanocomposites after cessation of UV irradiation. PLoS One 8(10):e75929
57. McEvoy JG, Cui W, Zhang Z (2013) Degradative and disinfective properties of carbon-doped anatase–rutile TiO2 mixtures under visible light irradiation. Catal Today 207:191–199
58. Asahi R (2001) Visible-light photocatalysis in nitrogen-doped titanium oxide. Science 293:26
59. Thakur N, Thakur N, Kumar K (2023) Phytochemically and PVP stabilized TiO2 nanospheres for enhanced photocatalytic and antioxidant efficiency. Mater Today Commun 35:105587
60. Yaaqoob LA, Noori AS, Atiyah HL et al (2025) Synergistic effect of bimetallic nanoparticles and evaluation as an antibacterial agent against *Streptococcus mutans* and *Klebsiella pneumonia*. Plasmonics. https://doi.org/10.1007/s11468-025-02811-0
61. Shirzadi-Ahodashti M et al (2023) Optimization and evaluation of anticancer, antifungal, catalytic, and antibacterial activities: biosynthesis of spherical-shaped gold nanoparticles using Pistacia vera hull extract (AuNPs@ PV). Arab J Chem 16(1):104423
62. Kadeřábková N, Mahmood AJ, Mavridou DA (2024) Antibiotic susceptibility testing using minimum inhibitory concentration (MIC) assays. NPJ Antimicrob Resist 2(1):37
63. Nabi G et al (2022) Green synthesis of TiO2 nanoparticles using lemon peel extract: their optical and photocatalytic properties. Int J Environ Anal Chem 102(2):434–442

Authors and Affiliations

Zainab Fakhri Merzah[1] · Zainab J. Shanan[2] · Nisreen Kh. Abdalameer[2] · Sokina Fakhry[3]

✉ Nisreen Kh. Abdalameer
nisreenka_phys@csw.uobaghdad.edu.iq

Zainab Fakhri Merzah
Zainab.fakhri@ilps.uobaghdad.edu.iq

Zainab J. Shanan
zainabjs_phys@csw.uobaghdad.edu.iq

Sokina Fakhry
sokinafahkry@yahoo.com

[1] Institute of Laser for Postgraduate Studies, University of Baghdad, Baghdad, Iraq

[2] Department of Physics, College of Science for Women, University of Baghdad, Baghdad, Iraq

[3] Al Furat Intermediate School for Girls, Ministry of Education, Babylon, Iraq